Turk Neurosurg 36(4):509-516, 2026
DOI: 10.5137/1019-5149.JTN.49331-25.2

Original Investigation

Neuro – Oncology

Received: 23.06.2025
Accepted: 16.11.2025
Published Online: 24.07.2026

Statistical Geometric Morphometric Shape Analysis of Ventricular Shape Changes in Giant Pituitary Adenomas Invading the Third Ventricle

Oguz ALTUNYUVA[1], Nur BALCIN[1], Gokhan OCAKOGLU[2], Mevlut Ozgur TASKAPILIOGLU[3], Selcuk YILMAZLAR[4]

[1]Bursa Cekirge State Hospital, Department of Neurosurgery, Bursa, Türkiye
[2]Bursa Uludag University Faculty of Medicine, Department of Biostatistics, Bursa, Türkiye
[3]Atlas University Faculty of Medicine, Department of Neurosurgery, Istanbul, Türkiye
[4]Bursa Uludag University Faculty of Medicine, Department of Neurosurgery, Bursa, Türkiye

Corresponding author: Mevlut Ozgur TASKAPILIOGLU ✉ mozgurt@gmail.com

ABSTRACT

AIM: To investigate the preoperative, early and late postoperative differences in the anterior callosal angle, lateral and third ventricle shapes of patients with pituitary macroadenoma operated via the transsphenoidal approach.

MATERIAL and METHODS: Shape data of the third and lateral ventricles were collected from the two-dimensional digital images. The generalised Procteus analysis was used to obtain mean shapes in the preoperative, early and late postoperative phases. The shape deformation of the ventricles from pre-to postoperative phases was evaluated using the thin plate spline method. Anterior callosal angle (ACA) was measured pre-to postoperative images and was analyzed statistically.

RESULTS: There was no significant lateral ventricle shape and ACA measurement difference in the pre and postoperative phases. The high-level deformations from the pre- to postoperative phase were seen in thin plate spline graphs. The highest deformation was observed at the third ventricle. Third ventricle deformation continued from the early to the late postoperative period, but this deformation is more limited than in preoperative comparisons.

CONCLUSION: We demonstrated that shape changes in the third ventricle of patients with pituitary macroadenoma persisted during the postoperative period through statistical geometric morphometric shape analysis. This phenomenon may result from dysfunction of the ventricular surface cilia due to chronic tumor compression and surgery-related neurotrauma. Additionally, we identified the diagnostic limitations of ACA in patients without radiological signs of hydrocephalus.

KEYWORDS: Anterior callosal angle, Statistical shape analysis, Pituitary adenoma, Third ventricle, Hydrocephalus

ABBREVIATIONS: EVDS: External ventricular drainage system, **VP:** Ventriculoperitoneal **MRI:** Magnetic resonance imaging, **CSF:** Cerebrospinal fluid, **PCA:** Principal component analysis, **TPS:** Thin plate spline, **GT:** Generalizability theory, **ACA:** Anterior callosal angle, **iNPH:** Idiopathic normal pressure hydrocephalus

Oguz ALTUNYUVA : 0000-0002-3450-0471
Nur BALCIN : 0000-0003-3928-8606
Gokhan OCAKOGLU : 0000-0002-1114-6051
Mevlut Ozgur TASKAPILIOGLU : 0000-0001-5472-9065
Selcuk YILMAZLAR : 0000-0003-3633-7919

INTRODUCTION

Pituitary adenomas are one of the most common brain tumors, accounting for 14% of all intracranial central nervous system tumors (10). Etiologically, these neoplasms are classified into functional (46%–64%) and non-functional (36%–54%) tumors (2,33). Although pituitary adenomas are histologically benign, especially the functional ones, they can lead to significant morbidities due to excessive hormone secretion and compression of surrounding neurovascular structures (5,6). Hence, early diagnosis and effective treatment are key to reducing morbidity and minimizing mortality.

Based on size, pituitary adenomas are classified into macroadenomas (>10 mm) and microadenomas (<10 mm) (6); however, those measuring ≥40 mm are defined as giant pituitary adenomas (11). In macroadenomas, mass effect is the most common finding, including visual disturbances; occasionally, hydrocephalus may be observed due to obstruction of the ventricular system and cranial nerves (15,31,35). It is known that tumors with suprasellar extension that destroy the floor of the third ventricle may lead to obstructive hydrocephalus (16–18).

With recent developments in imaging technologies and statistical modeling, it is possible to objectively assess changes in the shape of anatomical structures using landmark-based morphometric data. Anatomically significant reference points called "landmarks" can be translated using coordinate systems, making detecting subtle morphological differences through multivariate analysis possible. This is done using statistical shape analysis, a subfield of geometric morphometrics; this technique is increasingly becoming popular in clinical disciplines owing to its capacity to describe and visualize structural adaptations in anatomical features related to growth, pathology, or treatment. It has been applied to various anatomical regions, such as the sacroiliac joint, prostate, brainstem, and spine, effectively identifying disease-related structural variations and treatment-associated morphological changes (24–28,32,36). Likewise, existing studies suggest that shape-based evaluation methods may enhance our understanding of both pathological alterations and physiological adaptations in the female pelvis, contributing to obstetric risk assessment and surgical planning.

Accordingly, this study employed the landmark-based geometric morphometric method to investigate the preoperative and postoperative changes in ventricular morphology and radiological features in patients with giant pituitary adenomas who did not originally meet the radiological or clinical criteria for hydrocephalus.

MATERIAL and METHODS

Study Patients and Selection Criteria

We included patients who underwent tumor removal surgery for pituitary macroadenomas with suprasellar extension (Hardy-Vezina grades C and D) at the Department of Neurosurgery, Faculty of Medicine, Bursa Uludag University between September 2016 and March 2020.

In particular, patients with giant pituitary adenomas showing radiological evidence of third-ventricle indentation or partial intraluminal protrusion, without radiological or clinical signs of hydrocephalus, were considered for this study. Among these, patients with (i) Evans index of <0.30, (ii) absence of headache, papilledema, somnolence, or gait/cognitive disturbance, and (iii) no need for additional cerebrospinal fluid (CSF) diversion procedures, such as an external ventricular drain or a ventriculoperitoneal (VP) shunt, during follow-up, were included.

All included patients underwent contrast-enhanced pituitary magnetic resonance imaging (MRI) (Philips Achieva, Best, Netherlands; 3T scanner with 32-channel head coil) on three occasions: preoperatively, postoperative day 3, and six months postoperatively. Pre- and postoperative scans confirmed patent CSF pathways and third-ventricle indentation by the suprasellar tumor.

Ethical Considerations

The study was conducted in accordance with the principles of the Declaration of Helsinki. All participants provided informed consent before inclusion. Ethical approval for the study was obtained from the Bursa Uludag University local institutional review board (decision number: 2025/580-7/13, dated March 19, 2025).

Surgical Approach

All surgeries were performed by a single neurosurgeon using a binostril endoscopic endonasal transsphenoidal approach (EETA). Tumor removal was conducted without transventricular or intraventricular manipulation and without intentional ependymal violation. Standard multilayer skull-base reconstruction was used; no intra- or postoperative CSF diversion was required.

Collection of Two-Dimensional Ventricular Landmarks

Morphometric data were extracted from pre- and postoperative two-dimensional midsagittal MR images of all patients. We identified 14 anatomical landmarks that represent the shape of the lateral and third ventricles (Figure 1). Detailed definitions of these ventricular landmarks are provided in Table I. All landmarks were manually placed on each image using the TPSDIG 2.04 software.

Geometric Morphometric Analysis

Statistical shape analysis

The analysis focused on evaluating morphological changes in the lateral and third ventricles, which are anatomically interconnected through the foramen of Monro. In this context, we applied the generalized Procrustes analysis, a method known for minimizing the sum of squared differences between homologous landmarks, to obtain the mean shape and corresponding tangent coordinates of the ventricular system across the three time points (8). The tangent coordinates so obtained were then subjected to principal component analysis, and the resulting principal component scores were used for shape comparisons.

Pairwise comparisons were conducted between preoperative versus early postoperative (day 3), preoperative versus late

Table I: Descriptions of the Landmarks Used in the Study

Landmark No.	Definition	Landmark No.	Definition
1	Right ventricle's frontal horn	8	Right Rostrum of Corpus Callosum
2	Genu of Corpus Callosum	9	Right Stria Terminalis
3	Left ventricle's frontal horn	10	Head of right caudat nucleus
4	Head of left caudat nucleus	11	Roof of Third Ventricle
5	Left Stria Terminalis	12	Left side of Third Ventricle's floor
6	Left Rostrum of Corpus Callosum	13	Median side of Third Ventricle's floor
7	İnferior of Septum Pellucidum	14	Right side of Third Ventricle's floor

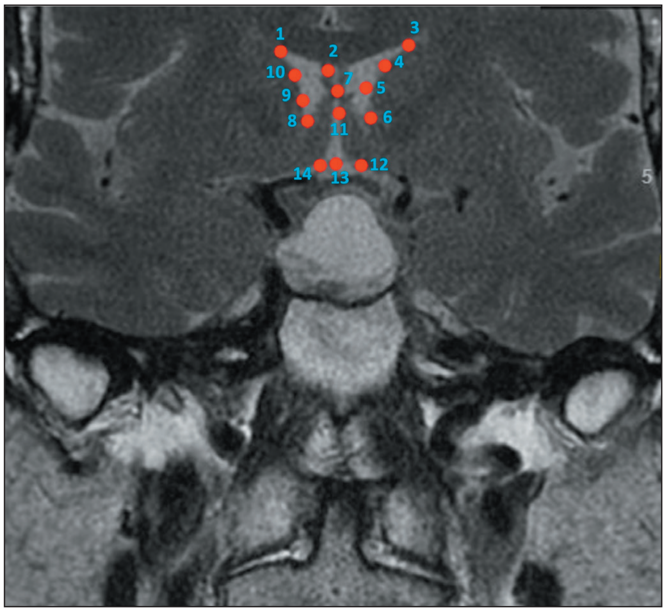

Figure 1: Landmark markings used for geometric morphometric analysis, targeting the sagittal plane of the ventricular system, including the third and lateral ventricles and their connection via the foramen of Monro, as visualized on coronal magnetic resonance imaging scans.

postoperative (six months), and early postoperative versus late postoperative periods using the multivariate paired Hotelling's T^2 test. Statistical significance was assessed using a Bonferroni-adjusted threshold of $\alpha/3 = 0.05/3 \approx 0.0167$ to control for type I error due to multiple comparisons. Shape deformation across the time points was further evaluated using the thin plate spline (TPS) method; regions showing the most prominent expansion or contraction were identified as the primary deformation zones. All analyses were performed using R software (34) and PAST software (12).

General statistical analysis

The anterior callosal angle (ACA; in degrees) was measured on coronal slices using the method described by Mantovani et al. (21). The normality of the distribution of angle measurements was assessed using the Shapiro-Wilk test, according to which the measurements for all three time points were normally distributed ($p > 0.05$). Therefore, descriptive statistics for these variables were expressed using mean ± standard deviation. To evaluate differences in measurements across the time points, a repeated measures analysis of variance (ANOVA) was used. Throughout the analysis process, the type I error rate was set at 5%. This analysis was performed using SPSS (IBM SPSS Statistics for Windows, version 25.0; IBM Corp., Armonk, NY).

Landmark reliability

Based on generalizability theory, the reliability coefficient (G) was calculated for a two-facet crossed design. The same researcher marked all landmarks; after two weeks, 10 randomly selected patients were re-marked by the same researcher to compute the G coefficient. The resulting G value reflected a high level of repeatability (G = 0.946). Calculations related to landmark reliability were performed using the calculator available at: http://biostat.home.uludag.edu.tr/landmark_reliability/G_coefficient.html.

RESULTS

The study included 25 patients (14 females and 11 males) with a mean age of 50.1 ± 14 years (range: 17–76 years) whose MRI data were used for geometric morphometric analysis.

The mean shapes of the third and lateral ventricles generated using Procrustes analysis were compared across the preoperative, early postoperative, and late postoperative periods in patients with giant pituitary adenomas (Figure 2). Pairwise comparisons revealed p-values of 0.048, 0.245, and 0.982 for the preoperative versus early postoperative period, preoperative versus late postoperative period, and early versus late postoperative period, respectively. Considering the Bonferroni-adjusted significance threshold due to multiple comparisons, none of these differences reached statistical significance.

The TPS analysis was performed using the mean shapes obtained from Procrustes analysis. Figure 3 illustrates the morphological changes observed between the preoperative and early postoperative periods in the region connecting the lateral and third ventricles. Figure 4 demonstrates the shape differences between the preoperative and late postoperative periods, and Figure 5 highlights the morphological changes

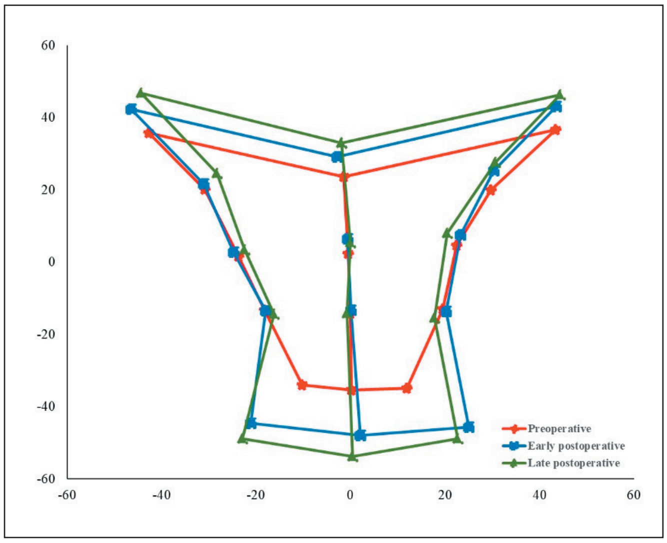

Figure 2: Procrustes mean shapes of the lateral and third ventricles, interconnected through the foramen of Monro, obtained from coronal magnetic resonance images in the preoperative, early postoperative, and late postoperative periods of patients with giant pituitary adenomas.

between the early and late postoperative periods. The TPS analysis visualizes shape deformations for each comparison, where the color gradient represents the degree of deformation; red and yellow regions indicate the highest degree of expansion, whereas blue regions indicate minimal change. In all analyses (Figures 3–5), the positions of the landmarks are indicated with black dots.

When the mean shapes and deformation maps were evaluated together, we observed marked morphological changes indicating expansion in the third ventricular region from the preoperative period to both early and late postoperative periods. Additionally, structural changes continued from the early to late postoperative period, although these changes were more limited compared to preoperative structures. A representative case demonstrating these temporal contour changes on coronal MRI is shown in Figure 6; it illustrates the progressive expansion-oriented deformation of the third ventricle, particularly around landmarks 11–14 identified in the morphometric model.

The mean ACA value was 140.98° ± 4.95° in the preoperative period, 140.06° ± 5.10° in the early postoperative period, and 139.46° ± 5.77° in the late postoperative period. For the re-

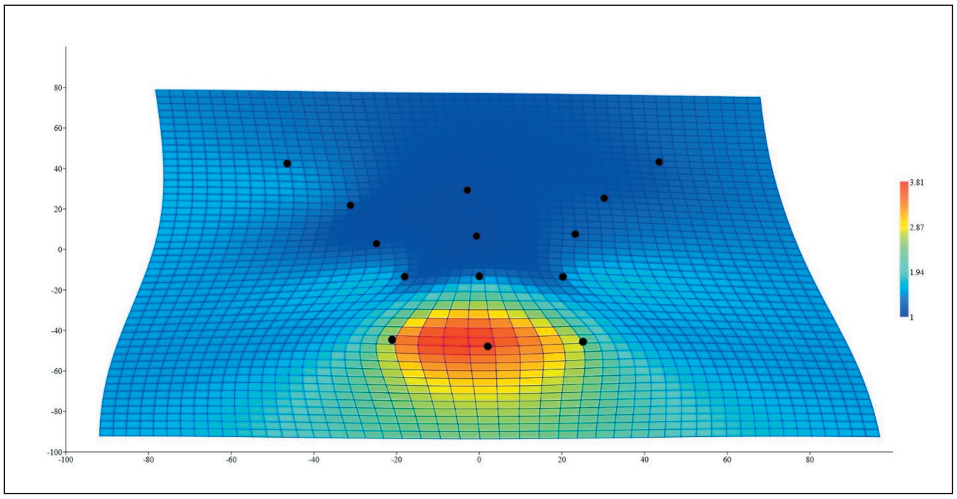

Figure 3: Thin plate spline analysis demonstrating the transformation of the mean shape of third ventricle region between the lateral and third ventricles from the preoperative to the early postoperative period.

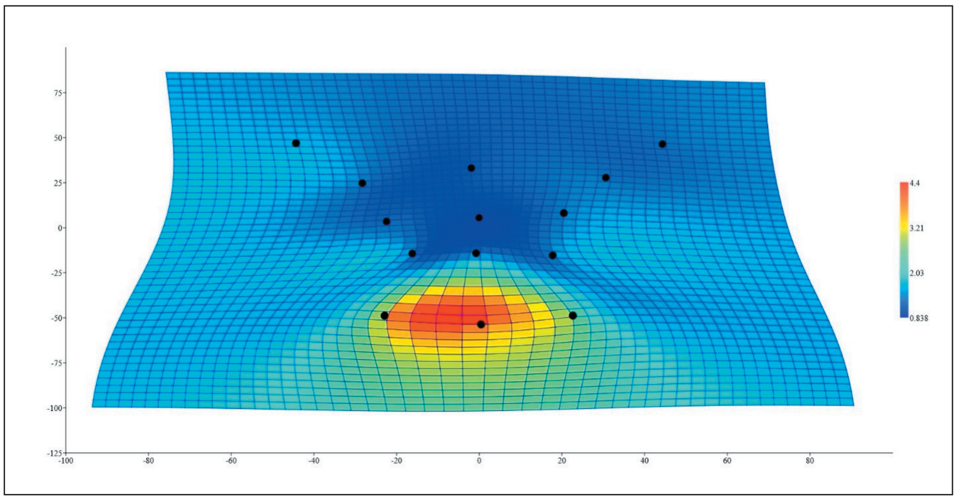

Figure 4: Thin plate spline analysis demonstrating the transformation of the mean shape of third ventricle region between the lateral and third ventricles from the preoperative to the late postoperative period.

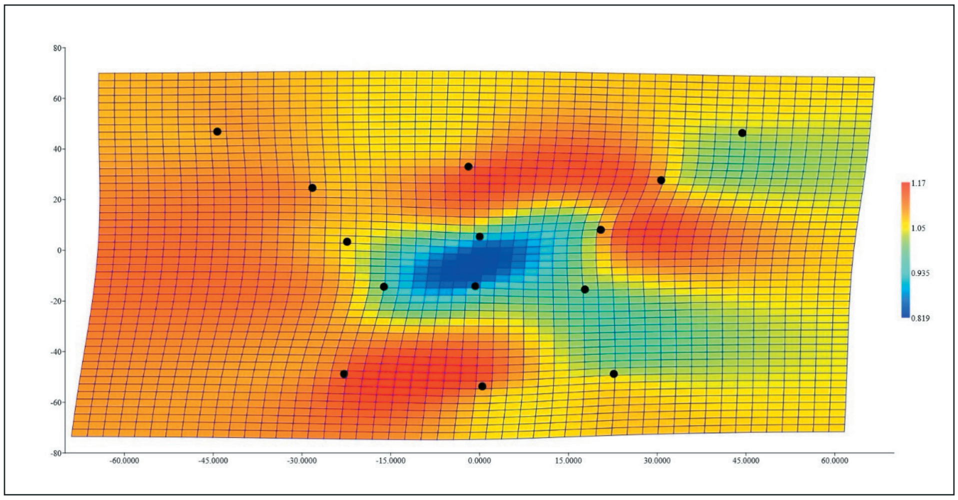

Figure 5: Thin plate spline analysis demonstrating the transformation of the mean shape of third ventricle region between the lateral and third ventricles from the early to the late postoperative period.

Figure 6: Representative case demonstrating the evolution of the third ventricle contour at three different time points on coronal magnetic resonance imaging (MRI) scans. **A)** Preoperative coronal T1-weighted image: A giant pituitary adenoma with suprasellar extension (asterisk) has invaded the third ventricle, nearly filling it. **B)** Early postoperative (day 3) coronal MRI: Following endoscopic endonasal decompression, the ventricle appears decompressed, the optic chiasm has returned to its normal position, and cerebrospinal fluid pathways are clearly re-established. **C)** Late postoperative (6-month) coronal MRI: The third ventricle exhibits a progressive, expansion-oriented contour deformation corresponding to landmarks 11, 12, 13, and 14 in the morphometric model (yellow arrows). Arrows indicate ventricular boundaries and areas of deformation.

peated measures ANOVA, the assumption of sphericity was considered acceptable (Huynh-Feldt epsilon value = 0.946). This test revealed no statistically significant main effect of time ($F = 1.47$, $p > 0.05$), indicating no significant change in the ACA across the three time points. Further trend analysis also revealed that neither the linear trend ($p = 0.154$) nor the quadratic trend ($p = 0.802$) was significant.

DISCUSSION

Hydrocephalus in pituitary macroadenomas can be observed both clinically and radiologically, and the condition can be monitored via radiological follow-up imaging (15,31,35). To the best of our knowledge, there is no prior study in the literature analyzing ventricular changes using geometric morphometric measurements in giant pituitary adenomas with third ventricular invasion. In our study, we wanted to address this issue and analyze the ventricular shape changes during the follow-up period. The patient cohort consisted of individuals without radiological signs of hydrocephalus (Evans index<0.3) who did not require additional cerebrospinal fluid diversion procedures (such as EVDS or VP shunting). Using statistical shape analysis, we evaluated morphological changes in the ventricular system during the preoperative, early postoperative, and late postoperative periods.

Tumors that completely occupy the third ventricle can obstruct the aqueduct of Sylvius, leading to hydrocephalus (17), whereas adenomas with a dumbbell-shaped growth pattern may obstruct the foramen of Monro, resulting in lateral ventricular enlargement (9). Our cases did not fully obstruct the foramen of Monro, showed no signs of increased intracranial pressure, and did not completely occupy the third ventricle. In our shape analysis, no significant deformation was observed at landmarks 1 through 10, which represent the lateral ventricles in coronal sections, across the preoperative, early postoperative, and late postoperative periods. Significant shape differences were particularly noted between the preoperative and early postoperative periods at landmarks 11, 12, 13, and 14, which define the boundaries of the third ventricle. Following the excision of the tumor that had invaded the third ventricle in the preoperative period, the ventricle was decompressed and refilled with CSF, resulting in changes in its morphology. Moreover, deformation was observed to persist in the direction of expansion from the early to late postoperative period (Figure 5).

According to the current hypothesis of CSF dynamics, CSF exhibits a pulsatile flow regulated by cerebral circulation and respiration (4,14). This flow is also supported by a constant microcurrent generated by motile cilia on the ventricular wall surface (37). Several studies have reported that dysfunction of these cilia can lead to ventricular enlargement (3,7,20,29). In acquired conditions such as viral infections, loss of cilia and gliosis along the ventricular walls may result in secondary hydrocephalus (1). For instance, Omran et al., in an experimental animal study, examined ciliary activity in the brains of mice with chronic alcohol consumption and detected hydrocephalus (30). The relationship between ciliary function and hydrocephalus has become a prominent research topic, supported by studies in rodent models demonstrating suppression of gliosis to prevent hydrocephalus (23), and genetic analyses examining ciliary function (13,19).

In our study, the continued deformation and expansion of the third ventricle from the early to late postoperative period may be explained by loss or reduction of ciliary function in the third ventricular ependyma due to chronic tumor compression/invasion and neurosurgical trauma. This may disrupt CSF flow dynamics, contributing to third ventricular dilation. The absence of shape change in the lateral ventricles, which were unaffected by either the tumor or surgical intervention, further supports the notion of localized third ventricular impact. However, the deformation in the direction of expansion continued in the late postoperative period in the 3rd ventricle, which was the area affected by the surgery and the tumor (Figure 5). Our shape analysis using geometric morphometric measurements supports this notion and represents the first such analysis on this topic in the literature.

This study also evaluated whether the anterior callosal angle (ACA) might serve as an early morphometric marker of CSF flow disturbance, even in patients without radiological hydrocephalus. Mantovani et al. suggested that ACA could be used to differentiate idiopathic normal pressure hydrocephalus (iNPH) from Alzheimer's disease, reporting that a value of ≤119° demonstrates high sensitivity and specificity for iNPH. The mean ACA value in healthy individuals was found to be 133.85° ± 5.86, and this value was significantly lower in iNPH patients (21). A subsequent study noted that ACA can also serve as a radiological parameter for monitoring the response to shunt surgery in iNPH patients (22). In our study, the mean ACA value in the preoperative period was 140.98° ± 4.95, with no significant change in the early (140.06° ± 5.10) and late postoperative periods (139.46° ± 5.77) ($F = 1.47$, $p > 0.05$). All values were well above the diagnostic threshold reported in the iNPH literature. All ACA values were consistent with those reported in healthy adults, and none of the patients met the criteria for hydrocephalus. We suggest that future large-scale, prospective studies investigate the utility of ACA not only in differentiating iNPH from Alzheimer's disease but also as a potential novel diagnostic parameter for hydrocephalus.

This study is the first to demonstrate the temporal shape changes of the ventricular system in by third ventricular invasion of giant pituitary adenomas using a landmark-based geometric morphometric method. Our findings suggest that ventricular deformation is not solely related to tumor excision, but may also be associated with postoperative alterations in CSF dynamics. Although no significant shape changes were observed in the lateral ventricles, the expansion-oriented deformation of the third ventricle persisted, which may be attributed to impaired cerebrospinal fluid dynamics secondary to ciliary dysfunction, as previously discussed.

Clinical Relevance of Non-hydrocephalic Shape Change

In the absence of radiological or clinical hydrocephalus, the observed third-ventricle deformation most likely reflects localized CSF–ependymal remodeling secondary to chronic suprasellar compression, rather than a global intracranial pressure elevation. Persistent expansion after decompression may further indicate ependymal ciliary dysfunction, as prolonged tumor indentation can alter cilia-mediated CSF propulsion and the mechanical compliance of the ventricular wall.

Given that all patients underwent endoscopic endonasal transsphenoidal surgery without transventricular manipulation, any direct operative contribution is expected to be minimal. Altogether, these findings support a local, cilia-driven biomechanical remodeling process rather than a pressure-driven hydrocephalic mechanism.

Accordingly, the landmark-based shape descriptors presented here should be regarded as physiomorphologic, subclinical markers, reflecting subtle CSF–ependymal interactions rather than symptomatic hydrocephalus. At present, these parameters are not proposed as diagnostic thresholds; instead, they may (i) provide quantitative monitoring of ventricular contour evolution after decompression and (ii) serve as hypothesis-generating variables for prospective studies correlating shape with neurocognitive outcomes, endocrine status, visual performance, and longitudinal CSF metrics. Elucidating these associations will be essential before any clinically actionable cut-points can be defined.

Limitations and Future Directions

This study has several limitations. It represents a single-center, retrospective series with a relatively small sample size, focusing exclusively on non-hydrocephalic giant pituitary adenomas with third-ventricle involvement. While this homogeneity minimizes confounders, it also limits the generalizability of our findings to other pathologies with more pronounced clinical sequelae, such as craniopharyngiomas, colloid cysts, or intraventricular metastases.

In addition, our analysis relied solely on two-dimensional pituitary MRI sections. Future prospective, multicenter studies involving larger cohorts and incorporating three-dimensional volumetric reconstructions and statistical geometric morphometric analyses may provide more comprehensive and reproducible insights.

Moreover, integrating such morphometric data with experimental animal models could contribute valuable mechanistic information about ependymal ciliary function and its role in ventricular shape remodeling. Collectively, these extensions will be essential to translate current physiomorphologic findings into clinically actionable and pathophysiologically grounded tools.

CONCLUSION

This study investigated ventricular shape alterations in patients with non-hydrocephalic pituitary macroadenomas treated via the transsphenoidal approach, utilizing a landmark-based geometric morphometric method across preoperative, early postoperative, and late postoperative time points. Additionally, it assessed the potential applicability of the anterior callosal angle (ACA)—a parameter traditionally used to differentiate idiopathic normal pressure hydrocephalus (iNPH) from Alzheimer's disease—in the diagnosis of non-hydrocephalic conditions. The observed persistent postoperative expansion-related deformation of the third ventricle may be attributed to ciliary dysfunction within the ventricular epithelium. We hope the findings of this study will inform and inspire future research in this field.

Declarations

Funding: This research did not receive any specific grant from funding agencies in the public, commercial, or not-for-profit sectors.

Availability of data and materials: The datasets generated and/or analyzed during the current study are available from the corresponding author by reasonable request.

Disclosure: The authors declare that there are no conflicts of interest related to this study.

AUTHORSHIP CONTRIBUTION

Study conception and design: MOT, GO
Data collection: OA
Analysis and interpretation of results: GO
Draft manuscript preparation: OA, NB
Critical revision of the article: MOT, GO, SY
Other (study supervision, fundings, materials, etc...): SY
All authors (OA, NB, GO, MOT, SY) reviewed the results and approved the final version of the manuscript.

REFERENCES

1. Afzelius BA: Cilia-related diseases. J Pathol 204:470–477, 2004. https://doi.org/10.1002/path.165
2. Agustsson TT, Baldvinsdottir T, Jonasson JG, Olafsdottir E, Steinthorsdottir V, Sigurdsson G, Thorsson AV, Carroll PV, Korbonits M, Benediktsson R: The epidemiology of pituitary adenomas in Iceland, 1995–2012: a nationwide population-based study. Eur J Endocrinol 173:655–664, 2015. https://doi.org/10.1530/EJE-15-0189
3. Banizs B, Pike MM, Millican CL, Ferguson WB, Komlosi P, Sheetz J, Bell PD, Schwiebert EM, Yoder BK: Dysfunctional cilia lead to altered ependyma and choroid plexus function, and result in the formation of hydrocephalus. Development 132:5329–5339, 2005. https://doi.org/10.1242/dev.02153
4. Bouzerar R, Tekaya I, Bouzerar R, Balédent O: Dynamics of hydrocephalus: A physical approach. Med Biol Eng Comput 50:251–266, 2012. https://doi.org/10.1007/s10867-011-9239-3
5. Clayton RN, Raskauskiene D, Reulen RC, Jones PW: Mortality and morbidity in Cushing's disease over 50 years in Stoke-on-Trent, UK: audit and meta-analysis of literature. J Clin Endocrinol Metab 96:632–642, 2011. https://doi.org/10.1210/jc.2010-1942
6. Dekkers OM, Biermasz NR, Pereira AM, Romijn JA, Vandenbroucke JP. Mortality in acromegaly: a metaanalysis. J Clin Endocrinol Metab. 1:61–67, 2008. https://doi.org/10.1210/jc.2007-1191
7. Del Bigio MR: Ependymal cells: biology and pathology. Acta Neuropathol 119:55–73, 2010. https://doi.org/10.1007/s00401-009-0624-y
8. Dryden IL, Mardia KV: Statistical Shape Analysis: With Applications in R, 2nd ed. Chichester: John Wiley & Sons, 2016. https://doi.org/10.1002/9781119072492
9. Garcia RJ, Maclachlan LR, Barber J, Ayvaz F, Amato D, Jayalath R, Ananthababu P, Olson: A retrospective cohort study assessing geometrical parameters related to visual deterioration in pituitary macroadenoma. J Clin Neurosci 107:1-7, 2023. https://doi.org/10.1016/j.jocn.2022.11.002
10. Gautam UM, Chacko AG: Management of hormone-secreting pituitary adenomas. Neuro Oncol 19:762–763, 2017. https://doi.org/10.1093/neuonc/now130
11. Golden N, Niryana W, Awyono S, Mardhika PE, Putra MB, Biondi: Transcranial approach as surgical treatment for giant pituitary adenoma during COVID-19 pandemic—what can we learn?: a case report. Interdiscip Neurosurg 25:101153, 2021. https://doi.org/10.1016/j.inat.2021.101153
12. Hammer Ø, Harper DAT, Ryan PD. PAST: Paleontological Statistics Software Package for Education and Data Analysis. Palaeontol Electronica. 1:1-9, 2001
13. Hasanain AA, Soliman MAR, Elwy R, Ezzat AM, Abdel-Bari SH, Marx S, Jenkins A, El Refaee E, Zohdi A: An eye on the future for defeating hydrocephalus, ciliary dyskinesia-related hydrocephalus: review article. Br J Neurosurg, 36:329-339, 2022. https://doi.org/10.1080/02688697.2022.2074373
14. Hladky SB, Barrand MA: Regulation of brain fluid volumes and pressures: basic principles, intracranial hypertension, ventriculomegaly and hydrocephalus. Fluids Barriers CNS, 21:57, 2024. https://doi.org/10.1186/s12987-024-00532-w
15. Iglesias P, Berrocal VR, Díez JJ: Giant pituitary adenoma: histological types, clinical features and therapeutic approaches. Endocrine 61:407–421, 2018. https://doi.org/10.1007/s12020-018-1645-x
16. Iwamura H, Nonaka M, Li Y, Ueno K, Takeda J, Hashiba T, Asai A: A case of acute hydrocephalus due to a giant prolactinoma rescued by transventricular neuroendoscopic tumorectomy. Surg Neurol Int. 14:30, 2023. https://doi.org/10.25259/SNI_1060_2022
17. Jamaluddin MA, Patel BK, George T, Gohil JA, Biradar HP, Kandregula S, Hv E, Nair P: Endoscopic endonasal approach for giant pituitary adenoma occupying the entire third ventricle: surgical results and a review of the literature. World Neurosurg 154:254-263, 2021. https://doi.org/10.1016/j.wneu.2021.07.022

18. Joshi SM, Chopra IS, Powell M: Hydrocephalus caused by giant pituitary tumors: case series and guidelines for management. Br J Neurosurg 23:595–601, 2009. https://doi.org/10.1080/02688690802535081
19. Kousi M, Katsanis N: The genetic basis of hydrocephalus. Annu Rev Neurosci 39:409–435, 2016. https://doi.org/0.1146/annurev-neuro-070815-014023
20. Lee L: Riding the wave of ependymal cilia: genetic susceptibility to hydrocephalus in primary ciliary dyskinesia. J Neurosci Res 91:1117–1132, 2013. https://doi.org/10.1002/jnr.23238,
21. Mantovani P, Albini-Riccioli L, Giannini G, Miletti D, Sorenson TJ, Stanzani-Maserati M, Oppi F, Elder BD, Cevoli S, Cortelli P, Palandri G: Anterior callosal angle: a new marker of idiopathic normal pressure hydrocephalus? World Neurosurg 139:548-552, 2020. https://doi.org/10.1016/j.wneu.2020.04.085
22. Mantovani P, Giannini G, Miletti D, Cevoli S, Valsecchi N, Gramegna LL, Albini-Riccioli L, Sturiale C, Cortelli P, Lanzino G, Elder BD, Palandri G, Pro-Hydro Study Group: Anterior callosal angle correlates with gait impairment and fall risk in iNPH patients. Acta Neurochir 163:749-766, 2021. https://doi.org/10.1007/s00701-020-04699-7
23. McAllister JP, Miller JM: Minocycline inhibits glial proliferation in the H-Tx rat model of congenital hydrocephalus. Cerebrospinal Fluid Res 27:7, 2010. https://doi.org/10.1186/1743-8454-7-7
24. Ocakoglu G, Baykal D, Altunyuva O, Taskapilioglu MO, Yilmazlar S: Statistical shape analysis of cerebellum in patients with Chiari malformation I. J Craniofac Surg 30:1683–1687, 2019. https://doi.org/10.1097/SCS.0000000000005505
25. Ocakoglu G, Ercan I: Traditional and modern morphometrics. Turkiye Klinikleri J Biostat 5:37–41, 2013.
26. Ocakoglu G, Taskapilioglu MO, Altunyuva O, Yilmazlar S: Statistical shape analyses of the brainstem in Chiari patients. Turk Neurosurg 4:618–622, 2021. https://doi.org/10.5137/1019-5149.JTN.32785-20.3.
27. Ocakoglu G, Taskapilioglu MO, Kaya IS, Akesen B, Dogan S: Statistical shape analyses of pediatric patients with scoliosis after surgical correction. Turk Neurosurg 33:252-257, 2023. https://doi.org/10.5137/1019-5149.JTN.38065-22.2
28. Ocakoglu G, Taskapilioglu MO, Kaya S, Yazici Z: Statistical shape analyses of patients with scaphocephaly after surgical remodeling. Turk Neurosurg 30:382–386, 2020. https://doi.org/10.5137/1019-5149.JTN.26387-19.2
29. Olstad EW, Ringers C, Hansen JN, Wens A, Brandt C, Wachten D, Yaksi E, Jurisch-Yaksi N: Ciliary beating compartmentalizes cerebrospinal fluid flow in the brain and regulates ventricular development. Curr Biol 29:229–241, 2019. https://doi.org/10.1016/j.cub.2018.11.059
30. Omran AJA, Saternos HC, Althobaiti YS, Wisner A, Sari Y, Nauli SM, AbouAlaiwi WA. Alcohol consumption impairs the ependymal cilia motility in the brain ventricles. Sci Rep. 1:13652, 2017. https://doi.org/10.1038/s41598-017-13947-3
31. Penn DL, Burke WT, Laws ER: Management of non-functioning pituitary adenomas: surgery. Pituitary 21:145–153, 2018. https://doi.org/10.1007/s11102-017-0854-2
32. Rahimli Ocakoglu S, Vatansever A, Atak Z, Yanardag N, Coskun BN, Akselim S, Ocakoglu G: Evaluation of sacroiliac joint shape in women with ankylosing spondylitis according to mode of birth delivery: a retrospective study. Medicina 61:39, 2025. https://doi.org/10.3390/medicina61010039
33. Rappana AK, Koivukangas J, Ebeling T, Pirila T: Incidence of pituitary adenomas in Northern Finland in 1992–2007. J Clin Endocrinol Metab 95:4268–4275, 2010. https://doi.org/0.1210/jc.2010-0537
34. Team RC: R: A language and environment for statistical computing. R Foundation for Statistical Computing, Vienna, Austria, 2014.
35. Vance ML: Pituitary adenoma: a clinician’s perspective. Endocr Pract 14:757–763, 2008. https://doi.org/10.4158/EP.14.6.757
36. Vatansever A, Yetemen M, Öngen G, Ocakoğlu G, Coşkun B: Characterizing prostate zonal shape changes associated with 5α-reductase inhibitors using MRI. Clin Anat, 37:815-820, 2024. https://doi.org/10.1002/ca.24218
37. Yamada S, Mase M: Cerebrospinal fluid production and absorption and ventricular enlargement mechanisms in hydrocephalus. Neurol Med 63:141–151, 2023. https://doi.org/10.2176/jns-nmc.2022-0331